Virus Research 320 (2022) 198901

Contents lists available at ScienceDirect

Virus Research

journal homepage: www.elsevier.com/locate/virusres

Novel RNA viruses from the native range of *Hymenoscyphus fraxineus,* the causal fungal agent of ash dieback

Wajeeha Shamsi [a,*], Hideki Kondo [b], Sven Ulrich [a], Daniel Rigling [a], Simone Prospero [a]

[a] Swiss Federal Institute for Forest, Snow and Landscape Research WSL, Zuercherstrasse 111, Birmensdorf 8903, Switzerland
[b] Institute of Plant Science and Resources, Okayama University, Kurashiki 710-0046, Japan

ARTICLE INFO

Keywords:
Invasive pathogens
Ash dieback
Mycovirus
Mitovirus
Circular RNA
Biological control

ABSTRACT

The native Japanese population of the fungus *Hymenoscyphus fraxineus*, the causal agent of ash dieback in Europe, was screened for viruses using a high-throughput sequencing method. Five RNA viruses were detected in 116 fungal isolates sequenced via Illumina RNA-seq platform, with an overall virus prevalence of 11.2%. The viruses were completely sequenced by RNA ligase mediated rapid amplification of cDNA ends (RLM-RACE) followed by Sanger sequencing. The sequences appear to represent new species from three established families (*Mito-*, *Endorna-* and *Partitiviridae*), one recognized genus (*Botybirnavirus*) and a negative-sense single-stranded RNA virus in the order *Bunyavirales* from the proposed family "Mybuviridae". The highest prevalence was found for the mitovirus (7.8%), that had two genomic forms (linear and circular), while the other viruses were detected each in one isolate. Co-infection of a mitovirus and an endornavirus was also observed in one of the infected isolates. Here we describe the molecular characterization of the identified viruses. This study expands the diversity of viruses in *H. fraxineus* and provides the basis for investigating the virus-mediated control of ash dieback in Europe.

1. Introduction

In recent years, significant advances in sequencing technologies have greatly accelerated the discovery of novel viruses in fungi and oomycetes (Botella et al., 2020; Sutela et al., 2019; Vainio et al., 2017). Since the first detection of a mycovirus in the cultivated mushroom *Agaricus bisporus* (Hollings, 1962), numerous mycoviruses have been reported in plant-associated fungi belonging to different ecological guilds, including saprotrophs, mycorrhizal fungi, endophytes and pathogens (Heinze, 2012; Marzano et al., 2016; Ruiz-Padilla et al., 2021). Prevalence of viruses in fungal species shows a strong variation, ranging from a few to more than 90 percent of the fungal individuals in a population being infected (Hillman et al., 2018).

With the increasing discovery of novel mycoviruses, the understanding of their origin and evolutionary history has also improved considerably (Koonin et al., 2015). Mycoviruses mostly have a double-stranded RNA (dsRNA) or a positive-sense single-stranded [(+)ssRNA] genome (Ghabrial et al., 2015). Negative-sense single-stranded RNA [(–)ssRNA] viruses have also been reported infecting different fungal genera (Donaire et al., 2016; Liu et al., 2014). Several studies have further investigated the diversity, lifestyles and genome structures of mycoviruses. Some examples include the discovery of (–)ssRNA viruses related to viruses of plants and animals (Donaire et al., 2016; Liu et al., 2009, 2014), the horizontal virus transfer from plant to fungal hosts (cucumber mosaic virus in *Rhizoctonia solani*) (Andika et al., 2017), the existence of capsidless (+)ssRNA viruses with mono- (yadokarivirus) and multipartite genome (hadakavirus) (Sato et al., 2020; Zhang et al., 2016a) and non-conventionally encapsidated dsRNA viruses (polymycoviruses) (Kotta-Loizou et al., 2022). Moreover, the discovery of circular ssDNA viruses (Bartholomäus et al., 2016; Donaire and Ayllón, 2017; Osaki et al., 2016; Yu et al., 2010) and a circular form of monopartite capsidless (+)ssRNA viruses, including the yeast narnavirus distantly related with mitoviruses and a yadokarivirus with a putative partner dsRNA virus (botybirnavirus) (Jia et al., 2022; Matsumoto et al., 1990), has expanded the description of mycoviruses beyond classical genome nature (Kondo et al., 2022).

A virus infection can be asymptomatic, beneficial or detrimental for the fungal host (Sutela et al., 2019). Mycoviruses, which have the potential to attenuate the pathogenicity of their host are of particular interest as biological control agents (Prospero et al., 2021). The best-known example is the successful biological control of chestnut blight with a (+)ssRNA mycovirus (Rigling and Prospero, 2018). In this

* Corresponding author.
E-mail address: wajeeha.shamsi@wsl.ch (W. Shamsi).

https://doi.org/10.1016/j.virusres.2022.198901
Received 15 July 2022; Received in revised form 22 August 2022; Accepted 24 August 2022
Available online 1 September 2022

specific case, the virulence and sporulation ability of the pathogen *Cryphonectria parasitica* (Murr). Barr. are reduced by Cryphonectria hypovirus 1 (CHV1, family *Hypoviridae*) (Choi and Nuss, 1992). Chestnut blight cankers can be treated therapeutically with virus-infected strains, allowing the tree to fight off the infection. Subsequently, the virus can spread and become established in a *C. parasitica* population (Prospero and Rigling, 2016). Although in the second half of the last century, the public interest in biological control has strongly increased because of greater environmental awareness in society, this possibility is still poorly applied to tree pathogens (Prospero et al., 2021). Developing a virus-mediated biological control system remains a long and laborious process involving several different steps (Prospero et al., 2021). An essential step of such process consists of screening native populations of the target fungal pathogen for parasitic mycoviruses (Rigling et al., 2021).

Ash dieback caused by the ascomycete *Hymenoscyphus fraxineus* (family Helotiaceae) is the most recent example of an invasive disease devasting European forests (Gross et al., 2014a). The fungus is native to East Asia where it occurs as a saprotrophic decomposer of leaves of local ash species (Zhao et al., 2013), and was presumably introduced to Europe in the early 1990s (Kowalski and Holdenrieder, 2009). On European ash tree species (*Fraxinus excelsior* and *F. angustifolia*), *H. fraxineus* induces necrotic lesions on leaves, twigs and stems, eventually leading to wilting and dieback of girdled shoots (Gross et al., 2014b). Necroses may also develop on the root collar of declining ash trees [e.g., Enderle et al. 2017]. Only a very little proportion of *F. excelsior* trees seems to be at least partially resistant to *H. fraxineus* (McKinney et al., 2014, 2011; Sollars et al., 2017) and to date, no effective control measures for ash dieback are available. In regard to biological control, several studies have explored *in vitro* the possibility to use leaf endophytes as antagonists for *H. fraxineus* (e.g., Halecker et al. 2020, Kosawang et al. 2018, Schlegel et al. 2016). Results, however, were rather inconclusive and did not lead to the development and implementation of field trials. Schoebel et al. (2014) identified a parasitic mycovirus (Hymenoscyphus fraxineus mitovirus 1, HfMV1; genus *Mitovirus*, a group of mitochondrially replicating viruses with capsidless (+)ssRNA genomes) in the European *H. fraxineus* population, which, however, does not seem to affect the virulence of its host (Lygis et al., 2017). Hence, HfMV1 is most likely not useful for the biological control of ash dieback.

In the present study, we screened a total of 116 *H. fraxineus* isolates from two native Japanese populations for mycoviruses using a high-throughput sequencing (HTS) approach. Specifically, we aimed at determining the prevalence of RNA viruses, exploring the mycoviral diversity and characterizing all detected viruses molecularly.

2. Materials and methods

2.1. Fungal isolates

A total of 116 isolates of *H. fraxineus* from two different geographic populations in Japan [Sugadaira, Nagano Prefecture and Hokkaido district, (Gross et al., 2014b)] were used (Table S1). The isolates were kept in the culture collection at WSL and were revived on diamalt agar (20 g/L Diamalt, Hefe Schweiz, Stettfurt, Switzerland; 15 g/L plant propagation agar, Condalab, Madrid, Spain) before analyses and incubated at room temperature in the dark for three to four weeks. The identity of the virus-infected isolates was reconfirmed by sequencing the Internal Transcribed Spacer (ITS) region by using primers ITS-1 and ITS-4 (Table S2) (White et al., 1990).

2.2. Total RNA and dsRNA extraction

For total RNA extraction, the *H. fraxineus* isolates were grown on Asolectin liquid medium [0.5% asolectin, 1.1 ml lactic acid, 1 mg thiamine, 62.5 ml Knop's solution (containing per L of water: 14.4 g calcium nitrate, 2.5 g potassium nitrate, 2.5 g magnesium sulphate, 2.5 g potassium dihydrogen phosphate) per L solution, pH 4.5]. The harvested mycelium was frozen in 2 ml tubes and after lyophilization 60 mg of it was used for total RNA extraction using Spectrum™ Plant Total RNA-Kit (Sigma-Aldrich). The RNA samples were pooled (31 samples in pool 1 and 3, 30 samples in pool 2, and 24 samples in pool 4) and sequenced (3.2 to 4.0 ug RNA was used for the library preparation) on the Illumina platform (Illumina TruSeq Stranded Total RNA library construction with Ribo-Zero treatment + NovaSeq 100 bp PE sequencing run; 100 M reads/sample) by Macrogen Inc. (Macrogen Europe). After RNA-sequencing (RNA-seq), the total of 116, 113, 106 and 102 million reads (101 nt paired-end reads) were obtained from the four pooled samples (namely the pool-1 to −4), respectively. Among these sequence reads, at least 83.3–86.7% of reads were mapped to the reference genome of *H. fraxineus* via a tool of the map read to refinance of CLC Genomics Workbench version 11 (CLC Bio-QIAGEN, Aarhus, Denmark) (McMullan et al., 2018) (supplementary file 1). The dsRNA extraction was performed by using the Double-RNA Viral dsRNA Extraction Mini Kit (iNtRON Biotechnologies, Seongnam-Si, Korea) and by a method using cellulose described previously (Eusebio-Cope and Suzuki, 2015).

2.3. Detection and sequencing of viral RNA

The sequence reads were assembled *de novo* using CLC Genomics Workbench version 11 (CLC Bio-QIAGEN). The assembled sequence contigs (pool-1 to −4: 30,312; 29,040; 30,412; 39,956 contigs, the host RNA sequences were not excluded) were subjected to screening for viral sequences, which was performed using the local Basic Local Alignment Search Tool (BLAST) with viral reference sequences from National Center for Biotechnology Information (NCBI, https://ncbi.nlm.nih.gov/). Virus-sequence-specific primers were designed using CLC Main Workbench version 7 (CLC Bio-QIAGEN) (Table S2) for the detection of viruses from each RNA pool by one-step Reverse Transcription (RT)-PCR method PrimeScript OneStep RT-PCR v2 (Takara Bio Europe SAS, Saint-Germain-en-Laye, France) as described previously (Urayama et al., 2014). Fungal actin gene primers of *H. fraxineus* (Table S2) were used as a positive control for RT-PCR (Schoebel et al., 2014). RNA-ligase-mediated rapid amplification of cDNA ends (RLM-RACE) was utilized to obtain the nucleotide sequences at the 5′ and 3′ termini following a protocol described by Jamal et al. (2019). The RACE-PCR products were ligated into pGEMT-Easy (Promega, Madison, WI, USA) and cloned into *Escherichia coli* DH5α competent cells (Takara Bio Inc., Shiga, Japan) for sequencing. Sequences of primers used in RLM-RACE are listed in Table S2. Any missing nucleotides within the sequence contigs were obtained by gap-filling RT-PCR by designing primers flanking the missing region (Table S2) followed by Sanger sequencing. The viral sequences reported in this study were deposited in Genbank/ENA/DDBJ database with accession numbers ON929979 to ON929989.

2.4. Characterization of RNA viruses

The open reading frame [ORF, 100 amino acid (aa) or longer] in each cDNA was detected using the NCBI ORF finder program (https://www.ncbi.nlm.nih.gov/orffinder/) with standard or yeast mitochondrial codon usage (as required). Sequence similarity searches were performed using the BLAST (BLASTx and BLASTp) programs from NCBI. The conserved domain database (CDD) (Marchler-Bauer et al., 2016) (http://www.ncbi.nlm.nih.gov/Structure/cdd/wrpsb.cgi) was used to search for conserved domains with the nucleotide sequences as queries.

To assign viruses to families and genera, phylogenetic analysis of the deduced polypeptides was performed based on the maximum likelihood (ML) method. Online MAFFT server (version 7) (https://mafft.cbrc.jp/alignment/server/) (Katoh and Toh, 2008) was used to align virus and virus-like sequences, and PhyML 3.0 to generate an ML tree with automatic smart model selection (SMS Model Selection) (Guindon et al.,

2010). Branch supports were calculated based on 1000 bootstrap repetitions. The tree was visualized using FigTree (version 1.4.4) (http://tree.bio.ed.ac.uk/software/).

Secondary structures at the 5′ and 3′ termini were predicted by RNA structure software (version 6.4) (Mathews et al., 2004) (https://rna.urmc.rochester.edu/RNAstructure.html). Amino acid sequences were aligned using the online CLUSTAL Omega tool to identify motifs in the deduced polypeptides.

2.5. Genome form of the new mitovirus

To verify a possible circular or concatenate nature of the genome of a mitovirus (see Results), two different approaches were used. First, a primer pair was designed spanning the 5′ and 3′ junction of the mitovirus (all the variants) (Table S2) and used to perform an inverse RT-PCR. Amplicons were subjected to Sanger sequencing and compared with the NGS-derived contig sequence. Second, total RNA of one *H. fraxineus* isolate infected with the mitovirus and one isolate infected with a (–)ssRNA virus (as a control of the linear type of RNA genomes, see Results) was treated with RNase R (Lucigen, Middleton, WI, USA) to remove linear RNAs. The reaction was set up by using 15 μg of the total RNA with 2 μl of 10 × reaction buffer in a 20 μl reaction. A total of 5 μl of the mix was collected as control from both samples followed by adding 10 units of Rnase R and incubation at 37 °C. Additional 5 μl of the solution were collected after 30 min, 60 min and 120 min. Rnase R was inactivated after each collection by incubating the solution at 80 °C for 5 mins. The untreated and treated samples, collected at all time points, were subjected to cDNA synthesis followed by PCR to detect the mitovirus infection.

3. Results

3.1. Diversity and prevalence of viruses in H. fraxineus populations

Local BLAST analysis of the sequence contigs assembled with the raw RNA-seq reads obtained by Illumina TruSeq revealed the presence of fourteen virus-like contigs in the 4 pooled samples (Table 1). These virus-like contigs showed sequence similarity to five RNA mycoviruses, including dsRNA viruses (botybirnavirid, partitivirid), (+)ssRNA viruses (mitovirid, endornavirid) and a (–)ssRNA virus (an unclassified taxon). Each putative viral-associated contig was assigned to host fungal isolate by RT-PCR analysis (Table S1). Three *H. fraxineus* isolates in the population Sugadaira and 10 in the population Hokkaido were found to be virus-infected, with an overall virus prevalence in the Japanese population of 11.2% (Table 2). We also screened 96 European *H. fraxineus* isolates from Switzerland and Lithuania (Lygis et al., 2017) from our culture collection at WSL for the five newly identified mycoviruses using RT-PCR with each of virus sequence-specific primers, but none of them was found to be virus positive (data not shown).

3.2. Genomic sequence of the identified viruses

Mitovirus. TruSeq data revealed five independent *de novo* assembled sequence contigs (contig name: p2-58, p2-59, p2-99, p4-130 and p3-1825) (Table 1 and supplementary file 2) with similarities to mitoviruses. These mitovirid-like contigs showed sufficient sequence heterogeneity to each other for building independent contigs (for details, see below), and only a few sequence variations within each contigs were detected from pooled samples (supplementary file 3). Although these sequence contigs showed almost similar 2.8k-nt in size, their terminal

Table 2
Prevalence of the five novel RNA viruses in the two Japanese populations of *Hymenoscyphus fraxineus*.

Virus	Family or genus	Population		
		Sugadaira, Nagano(N = 36)	Hokkaido(N = 80)	Overall(N = 116)
HfMV2	*Mitoviridae*	2	7	9 (7.75%)
HfEV1	*Endornaviridae*	0	1	1 (0.86%)
HfBV1	*Botybirnavirus*	1	0	1 (0.86%)
HfPV1	*Partitiviridae*	0	1	1 (0.86%)
HfNSRV1	"Mybuviridae"	0	1	1 (0.86%)
Total	–	3	10	13 (11.20%)

Table 1
BLASTp results of the polypeptides characterized in this study in two Japanese populations of *Hymenoscyphus fraxineus*.

Virus name (size)	Contig no.	Total read count*	Genome type or segment	Identity (%)	Cover (%)	BLASTp (top hit)	Accession number	Host fungal strain
HfMV2 (2822 nt)	p2-59	22,808	Circular / non-segmented linear	35.8	94	Ophiostoma mitovirus 7	AGT55877.1	*O. novo-ulmi* isolate (93–1224)
HfMV2-I (2819 nt)	p2-58	71,977	(Circular / non-segmented linear)	35.8	94	Ophiostoma mitovirus 7	AGT55877.1	*O. novo-ulmi* isolate (93–1224)
HfMV2-II (2823 nt)	p2-99	26,415	(Circular / non-segmented linear)	35.8	94	Ophiostoma mitovirus 7	AGT55877.1	*O. novo-ulmi* isolate (93–1224)
HfMV2-III (2821 nt)	p4-130	76,412	(Circular / non-segmented linear)	35.7	94	Ophiostoma mitovirus 7	AGT55877.1	*O. novo-ulmi* isolate (93–1224)
HfMV2-IV (2822 nt)	p3-1825	4435	(Circular / non-segmented linear)	35.5	94	Ophiostoma mitovirus 7	AGT55877.1	*O. novo-ulmi* isolate (93–1224)
HfEV1 (10,663 nt)	p3-3996	3013	Non- segmented	47.9	99	Sclerotinia sclerotiorum endornavirus 2	AND83000.1	*Sclerotinia sclerotiorum* isolate 11,691
HfBRV1 (6463 bp)	p1-219	183,182	dsRNA1	54.6	97	Sclerotinia sclerotiorum botybirnavirus 1-WX	QUE49161.1	*Sclerotinia sclerotiorum* Isolate 2017SS
(5714 bp)	p1-970	179,598	dsRNA2	53.2	92	Sclerotinia sclerotiorum botybirnavirus 1-WX	QUE49162.1	*Sclerotinia sclerotiorum* isolate 2017SS
HfPV1 (2440 bp)	p2-6573	3136	dsRNA1	64.6	96	Fusarium poae partitivirus 2	YP_009272947.1	*Fusarium poae* MAFF 240,374
(2150 bp)	p2-15588/ p2-11853	906	dsRNA2	44.7	92	Fusarium poae partitivirus 2	YP_009272948.1	*Fusarium poae* MAFF 240,374
HfNSRV1 (10,776 nt)	p3–1608	23,276	Non-segmented or segmented?	38.5	85	Botrytis cinerea negative stranded RNA virus 9	QKW91263.1	*Botrytis cinerea* BCS8_DN5169

* : the number of raw reads mapping to the virus sequences were obtained by the Read Mapping algorithm via CLC Genomic Workbench with following parameters: length fraction = 0.75; and similarity fraction = 0.95. The mapping results were also included in supplementary file 2.

regions all have totally different locations (supplementary file 4). The detailed analyses of the mitovirid contigs suggested that the sequence was connected head to tail in the termini and different breaking points, which may occur during the sequence assembly, were estimated for each of them (Fig. S1a and supplementary file 5). The RLM-RACE with primer sets near the putative 3′-/5′ junction provided the potential 3′- and 5′-end sequences of this mitovirus from the fungal strain R1153 (the contig p2–59) [3 clones each]. Based on the sequence alignments, the adjacent sides of putative 3′-/5′ junction regions were well conserved among the contig sequences, except for the five nucleotides at the expected 5′ termini (Fig. S1b and supplementary file 6). Note that we could not get consensus results in the preliminary RLM-RACE analyses, which were conducted with the primers more distantly located at the expected termini, due to unknown reasons (data not shown). The missing sequences at the breaking points in each contig were also determined by using gap-filling RT-PCR. The obtained mitovirid-like sequence contigs shared 92.4–94.3% and 94.2–96.9% identity with nucleotide and amino acid sequences, respectively (Fig. S1c) and were thus considered as variants of the same mitovirid. Nine out of 116 *H. fraxineus* isolates were infected with this mitovirid or its four variants (Table 2 and S1). The dsRNA of the viruses was not detected on agarose gel, probably due to low accumulation of the replicative intermediate form (dsRNA, data not shown). The virus was clearly different from the previously described Hymenoscyphus fraxineus mitovirus 1 (Schoebel et al., 2014) (see below) and was therefore named Hymenoscyphus fraxineus mitovirus 2 (HfMV2) (Fig. 1B). The four other HfMV2 variants were designated HfMV2-I to HfMV2-IV (Table 1).

HfMV2 (+)ssRNA genome was 2822 nucleotide (nt) in length and predicted to encode for two ORFs- a long ORF of 710 aa in length (molecular mass 83.1 kDa) and a reverse ORF of 120 aa in length, when mitochondrial codon usage is applied. Among the other variants, shorter ORFs (<100 aa) were predicted with different locations in the 5′-UTRs, suggesting these small ORF cistrons may not be well conserved in the genome (data not shown). The long ORF encoded protein has a signature of the RNA-dependent RNA polymerase (RdRP) domain (Mitovir_RNA_pol, pfam05919) at nt position 1369–2181 (Fig. 1A), while the reverse ORF protein showed no hits with known proteins. All six conserved motifs characteristic of mitovirids (including the key motif GDD) were present in the putative RdRPs of HfMV2 and other reported mitoviruses (Fig. S2). HfMV2 RdRP showed ~35% identity in BLASTp to those of Ophiostoma mitovirus 7 (OnuMV7) and Grapevine-associated mitovirus 13 and 14 (Table 1). Phylogenetic analysis based on the deduced amino acid sequences of RdRPs suggested that HfMV2 belonged to the newly established genus *Kvaramitovirus* in the family *Mitoviridae* (Fig. 1B). The species demarcation criteria for mitovirids have recently been updated (<70% identity in RdRP regardless of whether assigned to the same or different host species) (https://talk.ictvonline.org/files/ictv_official_taxonomy_updates_since_the_8th_repor

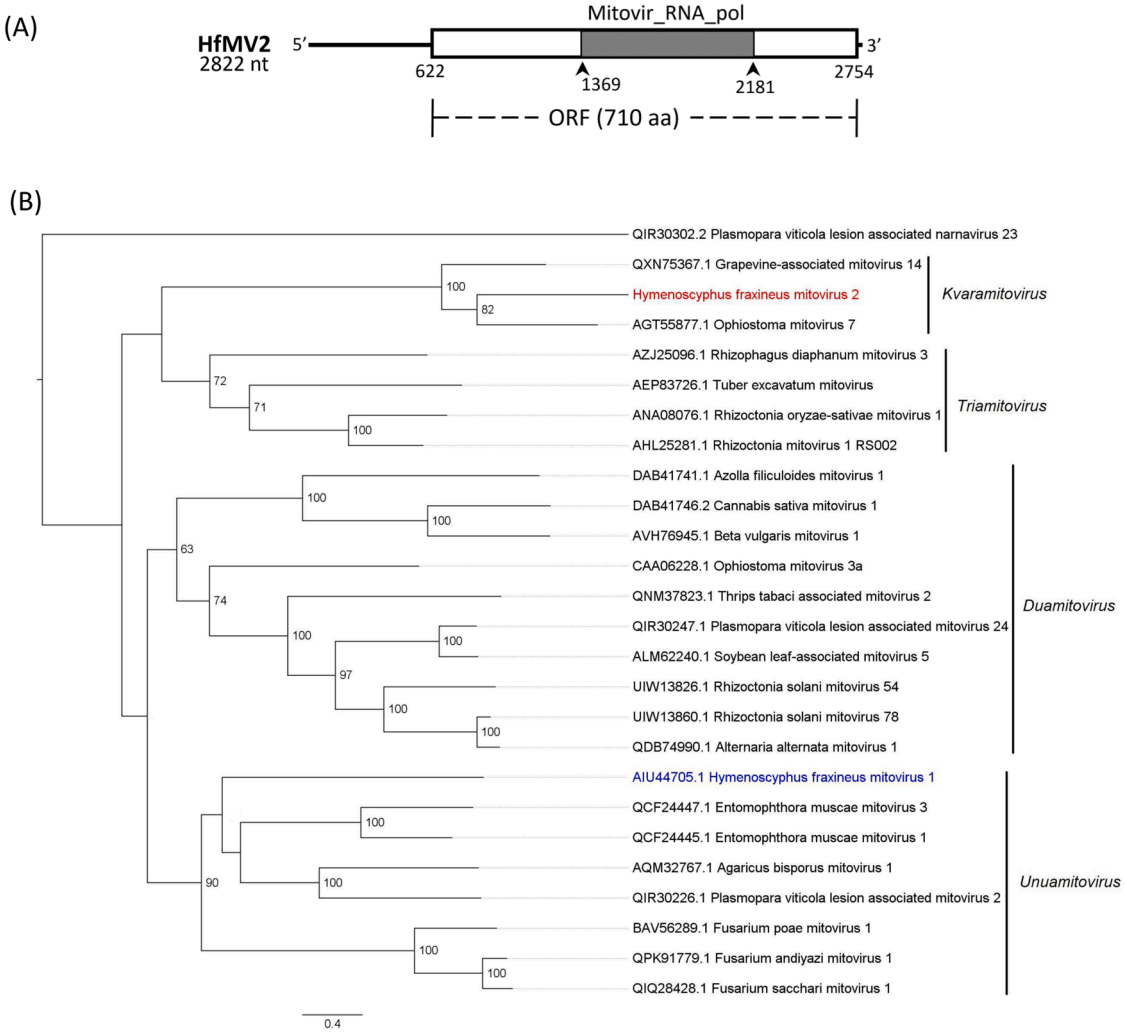

Fig. 1. (A) Schematic representation of the novel mitovirus HfMV2. The ORF is represented in white and the RdRP domain in gray. (B) Phylogenetic analysis based on RdRP of HfMV2. Maximum-likelihood tree was generated based on the amino acid alignment of the deduced ORF. Numbers at nodes are bootstrap values out of 1000 replicates. Narnavirus is used as an outgroup to root the tree. Bootstrap values (%) less than 60 are not shown.

t/m/fungal-official/13289), and thus, HfMV2 could be considered to represent a new virus in the genus *Kvaramitovirus*.

The mitovirid contig sequences via *de novo* assembly showed a feature of the head-to-tail connection of the genomic termini suggesting the existence of a connected genomic RNA terminus, as mentioned above (Fig. S1a and b). Thus, we assumed that either the mitovirid RNA was forming a dimer or had a circular form. To test the hypothesis, an inverse RT-PCR was carried out by designing the forward primer upstream of the stop codon and the reverse primer close to the start codon (Fig. 2A). A PCR product of about 900 bp in size was obtained (Fig. 2B), and Sanger sequences verified the junction of the 3′ and 5′ termini of the genome (Fig. 2C), suggesting the genome has two potential RNA natures with a circular or concatemer form along with the monomer. To further verify the circular or concatemer nature of this virus, total RNA was subjected to linear ssRNA-specific RNase R treatment. After digestion with RNase R, the (–)ssRNA virus with a putative linear RNA genome used as a control was not detected anymore, while HfMV2 could be found both with the primer sets for conventional and inverse RT-PCR (Fig. 2D), confirming the presence of at least the circular RNA form.

Endornavirus. In the RNA-seq data, a sequence contig (contig name p3–3996) related to endornaviruses (family *Endornaviridae*) was identified (Table 1). One fungal isolate (strain R0964) from the population Hokkaido was tested positive for this virus (Table S1). The same isolate was found to be coinfected with HfMV2-V. The complete sequence of (+) ssRNA genome was 10,663 nt in length. BLASTn search indicated an identity of ~70% with known endornaviruses with a query cover of 30% (data not shown), while BLASTp search indicated an identity of ~48% with Sclerotinia sclerotiorum endornaviruses with a query cover of 99% (e-value= 0) (Table 1) and other members of the genus *Betaendornavirus*. The virus was named *Hymenoscyphus fraxineus* endornavirus 1 (HfEV1).

A single large ORF (3539 aa, molecular mass 395.1 kDa) was encoded by HfEV1 with several conserved domains including the methyl transferase (MTR, Vmethyltransf superfamily; pfam01660; E-value = $3.7e^{-10}$), DEAD like helicase superfamily domain (DEXDc smart00487; E-value = $5.6e^{-14}$), RNA helicase (Hel, Viral RNA Helicase superfamily I; pfam01433; E-value = $4.0e^{-12}$) and RdRP domain (RdRP_2 superfamily; pfam 00,978; E-value = $1.3e^{-16}$). An additional HrpA superfamily domain (HrpA-like RNA helicase; cl34328; E-value = $1.7e^{-03}$) was predicted overlapping the DExH domain at the N-terminal (Fig. 3A) which is involved in translation, ribosomal structure and biogenesis. The ORF protein also contained a cysteine-rich region (CRR) at aa position 781–849 (Figs. 3a and S3a). HfEV1 had sequence properties similar to previously reported endornaviruses, which include the presence of two CxCC signatures in the CRR as shown in the multiple sequence alignment of HfEV1 and reported endornaviruses (Fig. S3b), short 5′ and 3′ UTRs of 11 and 32 nt in length, respectively, and a poly C sequence at the 3′ end (Fig. S3c), indicating the sequence is complete.

At the N-terminus of the polypeptide, an MTR domain was present (nt position 825–1493) containing the conserved motifs I to IV (Fig. S4a). Analogous to the SsEV1, the motifs I, II and IV contained conserved histidine residues, the signature sequence DxxR (DNAR) and conserved tyrosine residue, respectively. The DExH (HrpA-like) domain was identified at nt position 3723–4148 (4041–4595) and contained I–V motif (Fig. S4b). The Hel domain was present at nt position 5460–6161 and all the conserved motifs (I-VI) that are characteristic of the superfamily 1 and 2 of helicase were detected in this domain (Fig. S4c). The RdRP domain was located in the C-terminal region (nt position 9597–10,097) having the conserved motifs typical to endornaviruses (Fig. S4d). The protein sequence of individual domains was subjected to BLASTp search and maximum likelihood trees were generated for the RdRP, MTR, DExH/Hrp-A and HELdomains. Qualitatively similar results were observed for all domains, with HfEV1 clustering with other betaendornaviruses (Figs. 3b and S5a–c).

Together, all these findings with the ICTV species demarcation criteria for betaendornaviruses (overall nucleotide sequence identity below 75%) (Valverde et al., 2019), supported that HfEV1 is a virus belonging to the genus *Betaendornavirus*.

Botybirnavirus. Two virus-like contigs (contig name, p1-219 and p1-970) from the RNA-seq data showed similarity to botybirnaviruses (genus *Botybirnavirus*) (Table 1) and RT-PCR revealed that only one isolate (strain R1158) from the population of Sugadaira was infected with this virus (Table S1). These sequence contigs were assumed to represent the two dsRNA segments of a botybirnavirus. The larger segment was designated dsRNA1 and the smaller one as dsRNA2. The

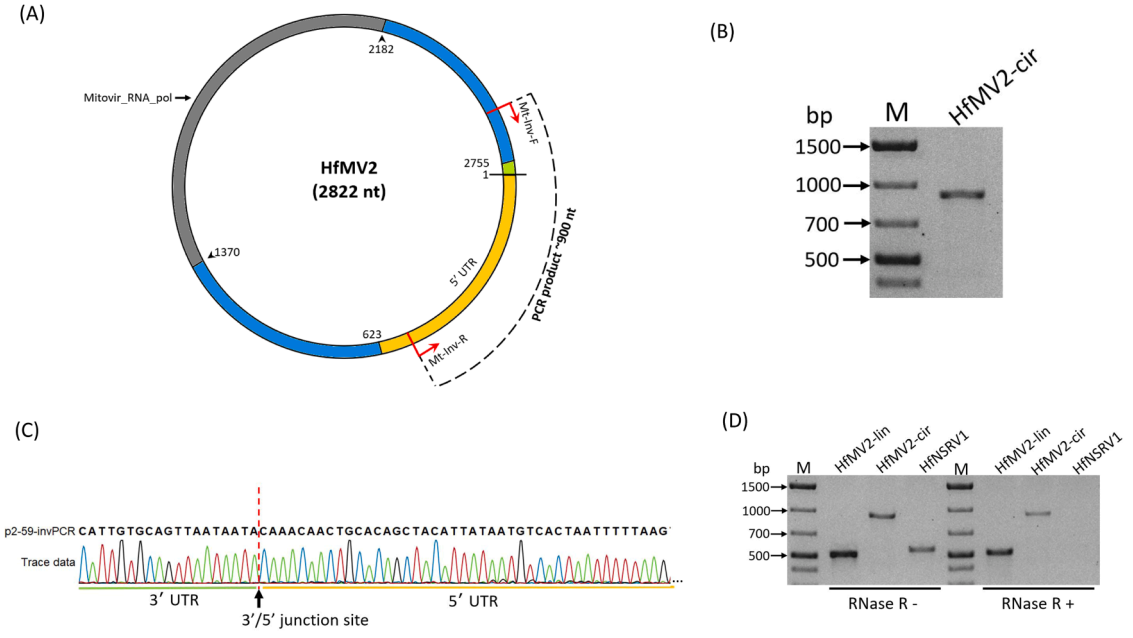

Fig. 2. (A) Schematic representation of the circular genomic form of HfMV2. The positions of the primers used for inverse RT-PCR to verify the circular genome are marked with red arrows. (B) Inverse RT-PCR results of the circular genome of HfMV2. The total RNA of isolate R1153 was used as a template for reverse transcription. (C) Sanger sequencing chromatogram of inverse RT-PCR product confirmed the 5′ and 3′ junction of HfMV2. (D) RT-PCR results of RNase R untreated and treated total RNAs of isolate R1153 (p2–59) confirming the circular genome of HfMV2. lin, linear; cir, circular.

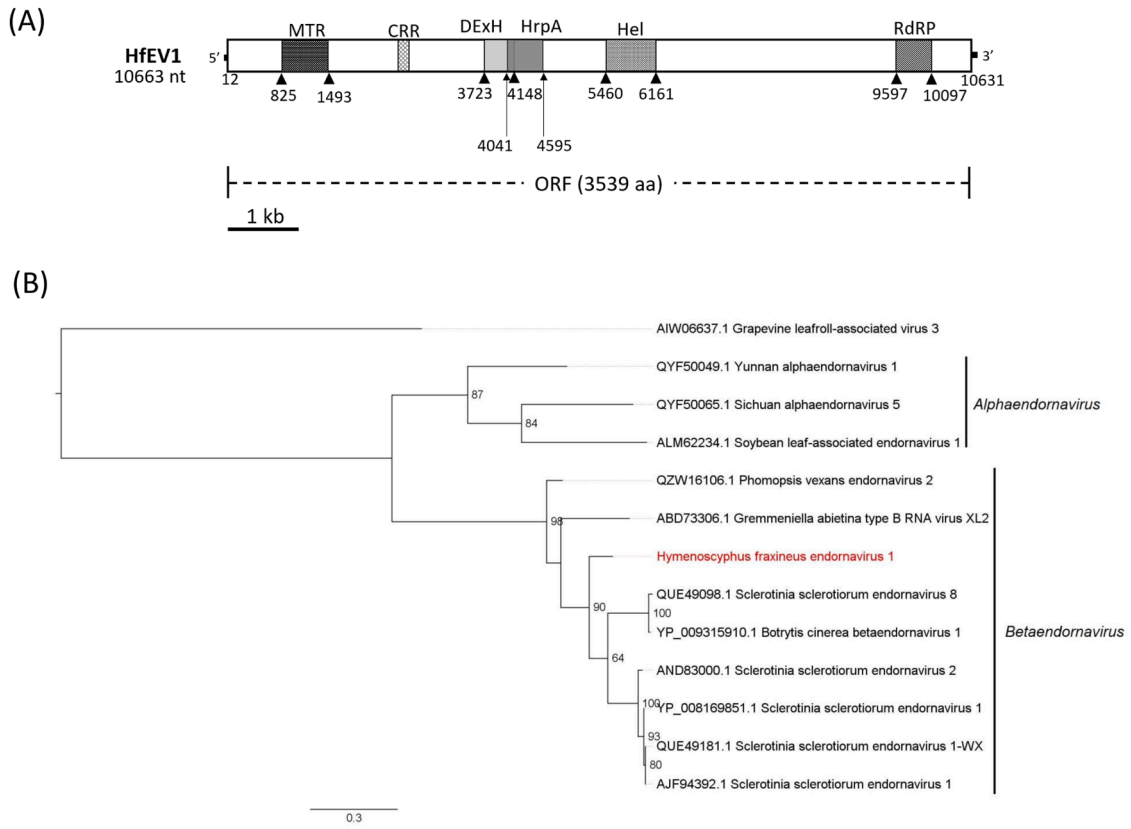

Fig. 3. (A) Schematic representation of genome organization of HfEV1. The ORF is represented in white and the shaded blocks represent the conserved domains, cysteine rich region (CRR), Metyltransferase (MTR), DExH/Hrp_A, Helicase (Hel) and RdRP. (B) Maximum-likelihood phylogenetic analysis based on RdRP domain of HfEV1. Numbers at nodes are bootstrap values out of 1000 replicates. Grapevine leafroll-associated virus (a plant closterovirus) was used as outgroup to root the tree. Bootstrap values (%) less than 60 are not shown.

complete sequence of the two segments was obtained by conducting RLM-RACE with Sanger sequencing using total RNA fraction.

The dsRNA1 and dsRNA2 were 6463 bp and 5714 bp in length, respectively. Both the dsRNAs encoded for a single large ORF in their positive strands. The ORF1 (encoded by dsRNA1) was 1947 aa in length (molecular mass ~220.9 kDa) (Fig. 4A) and a conserved domain for RdRP (RT_like superfamily; pfam 02123) was found at nt position 4244–5434, along with all eight conserved motifs characteristic of botybirnaviruses (Fig. S6a). The ORF2 (encoded by dsRNA2) was 1705 aa in length (molecular mass 189.2 kDa) (Fig. 4A) and no conserved domains were detected in it. The 5′ UTRs of the positive strands of dsRNA1 and dsRNA2 were 514 and 488 nt in length, whereas the 3′ UTRs were 105 and 108 nt in length, respectively (Fig. 2a). Alignments of the 5′ and 3′ UTRs of the two dsRNAs showed high sequence identity of 85.4% and 70.2%, respectively, with strictly conserved nucleotides at both termini (Fig S6b and c). Additionally, stem-loop structures were also predicted at the 5′ and 3′ termini of positive stands of both dsRNAs (Fig S6d).

BLASTp search of the ORF1 protein revealed ~54% identity with the polyprotein of Sclerotinia sclerotiorum botybirnaviruses (SsBRV1) and Botryosphaeria dothidea botybirnavirus 1. The polypeptide encoded by ORF2 showed ~52% identity to a hypothetical protein of the same viruses (Table 1). The 5′ and 3′ UTRs also showed significant similarity to the SsBRV1 (data not shown). Phylogenetic analysis of the ORF1 deduced polypeptides confirmed a close relation of this botybirnavirus to the members of the genus *Botybirnavirus* (Fig. 4B). These data suggested that the botybirnavirus might belong to a new species, although the species demarcation criteria have not been defined for the genus. We have thus tentatively named it Hymenoscyphus fraxineus botybirnavirus 1 (HfBRV1).

An alignable region was detected between the polypeptides encoded by HfBRV1 with significant similarity (E-value = $2e^{-13}$) at aa position 364 to 824 of ORF1 encoded polypeptide and aa position 128 to 615 of ORF2 encoded polypeptide (Fig. S7a). A similar topology was observed when the phylogenetic analysis was done with the alignable regions of the two ORFs (Fig. S7b and see discussion).

Partitivirus. Paritivirus-like contigs (contig name, p2-6573, p2-15588, p2-11853, p2-18448 and p2-8068) were detected in the RNA-seq data (Table 1 and data not shown). The larger contig (p2-6573) was similar to partitivirus dsRNA and the four smaller contigs derived from the two putative variants of dsRNA2. A single isolate (strain R1006) from the population Hokkaido was positive for this virus (Table S1). To obtain the full-length sequence of the dsRNA segments, RLM-RACE was performed, followed by Sanger sequencing. Two contigs (p2–15588 and p2-11853) were derived from the same dsRNA2 segment and thus they have concatenated as the single contig (p-15588/11853) for further analyses. Two dsRNA segments corresponding to contigs p2–6573 (dsRNA1) and p-15588/11853 (dsRNA2) encoded a single large ORF (ORF1 and 2, respectively). The ORF1 encoded an 88.5 kDa protein (putative RdRP of 756 aa), while the ORF2 a 71.6 kDa protein (putative capsid protein, CP of 652 aa) (Fig. 5A). The putative dsRNA segment of the partitivirus (a possible dsRNA2 variant: contig p2–18448, along with the possible partner p2–8068) was also detected in the same isolate by RT-PCR, but we were unsuccessful in obtaining its termini by RLM-RACE (data not shown and see discussion). The virus was named Hymenoscyphus fraxineus partitivirus 1 (HfPV1). The dsRNA1 and dsRNA2 were 2440 bp and 2150 bp long, respectively, which correspond to the lengths of *Betapartitivirus* species. BLASTp search showed that the two dsRNAs showed moderate sequence identity (44 to 64%) with Fusarium poae partitivirus 2 (FpPV2) (Table 1). The reconstructed CP of the putative

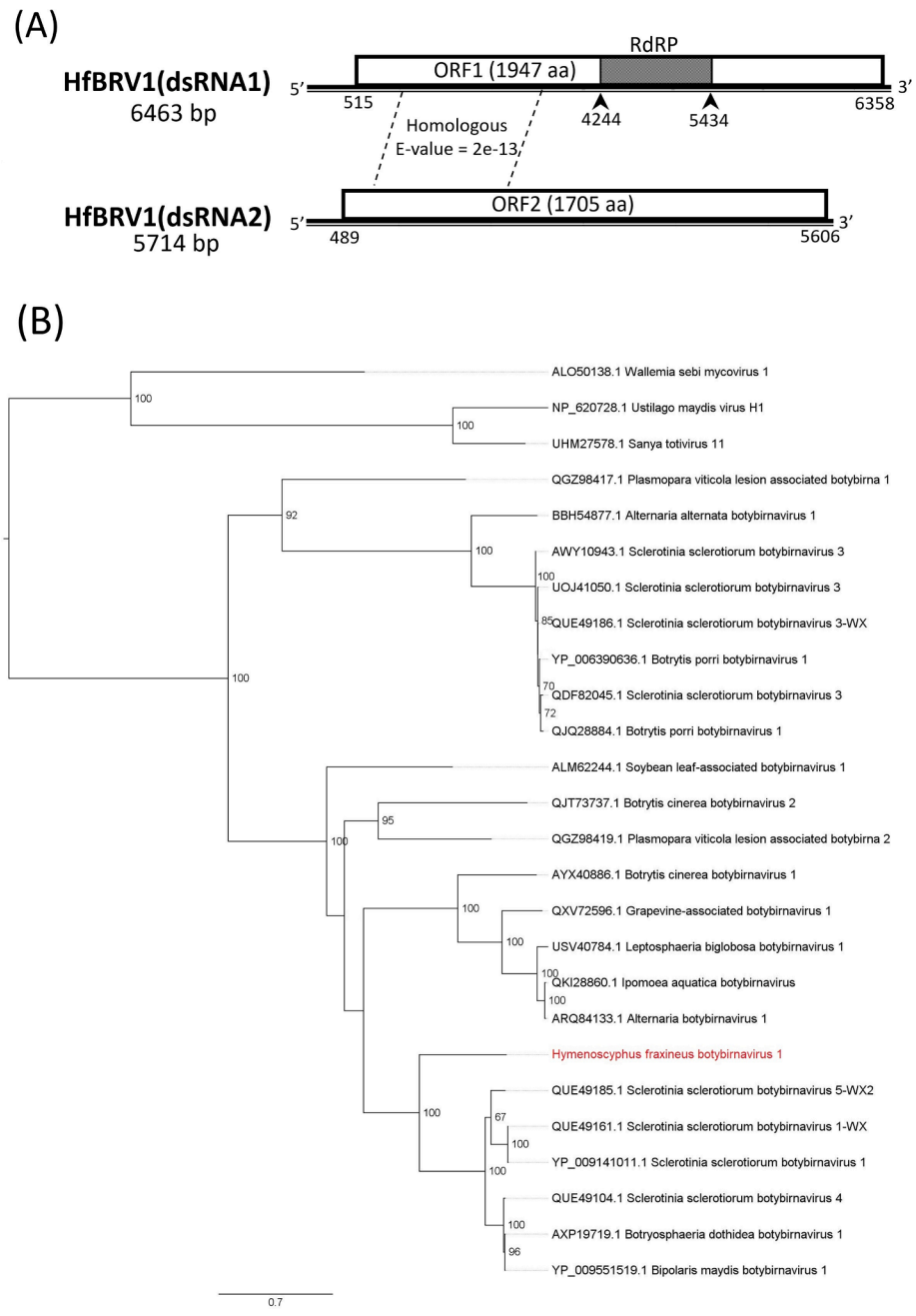

Fig. 4. (A) Genomic organization of the HfBRV1 with a bi-segmented dsRNA. The positive strand of the dsRNA1 includes a 514-nt 5′ UTR, an ORF1 encoding 1947 aa protein and a 105-nt 3′ UTR. An RdRP domain was present at nt positions 4244–5434. The positive strand of the dsRNA2 includes a 488-nt 5′ UTR, an ORF2 encoding 1705 aa protein and a 108-nt 3′ UTR. A potential duplicated region of the structural proteins showing a moderate aa identity is represented by dotted lines. (B) Phylogenetic analysis of HfBRV1. Maximum-likelihood tree based on RNA-dependent RNA polymerase of HfBRV1. Numbers at nodes are bootstrap values out of 1000 replicates. Bootstrap values (%) less than 60 are not shown.

second dsRNA2 variant (p2-18448 and p2-8068 with a gap region) shared 40.0% and 47.8% (query coverage 72%) identities with the CP of the first variant and FpPV2, respectively (data not sown), but still need to verify whether the variant (two contigs) is a part of the partitivirus. Similar relationships between viruses were observed in the RdRP-based phylogenetic tree of HfPV1 (Fig. 5B).

Several conserved motifs were obtained in the RdRP-based sequence alignment with other partitiviruses (Fig. S8a). Alignment of the 5′-end indicated conservation of 19 out of 20 nucleotides (Fig. S8b) and an interrupted poly A-tail at the 3′-end of both the dsRNAs. Additionally, a stem-loop structure was predicted at both the 5′ and 3′ termini of both RNAs (Fig. S8c). These findings, together with the ICTV species demarcation criteria for betapartitiviruses (≤90% aa identity in RdRP, ≤80% aa identity in CP) (Vainio et al., 2018), suggested that HfPV1 is a novel member in the genus *Betapartitivirus*.

Negative stranded RNA virus. A virus-like sequence (contig name, p3–1608) from the RNA-seq data was related to the viruses of order *Bunyavirales* from the phylum *Negarnaviricota* (Table 1). A single isolate (strain R1157) from the population Hokkaido was tested positive for this virus-like agent (Table S1). Based on RLM-RACE, the complete sequence of this virus was 10,776 nt in length and encoded a single ORF (L protein) of 419.9 kDa (3572 aa in length) (Fig. 6A). The virus L protein showed 38–40% identity to those of the Botrytis cinerea negative stranded RNA virus 1, −2, −6 and −8–11 (BcNSRV1, 2, 6, 8–11).

A conserved domain for RdRP (Bunya_RdRP superfamily; pfam04196) in the L protein was detected at nt position 5581–6555 (Fig. 6A). Alignment of the RdRP with closely related sequences showed the presence of all the five conserved motifs A to E, along with the pre-motif A (Fig. S9a), representing the highly conserved RdRP regions of the family *Bunyaviridae*. HfNSRV1 had a short 5′-terminal of only six nucleotides and the 3′-terminal consisted of 51 nucleotides (Fig. 6A).

The phylogenetic tree of the deduced polypeptide (L protein) of

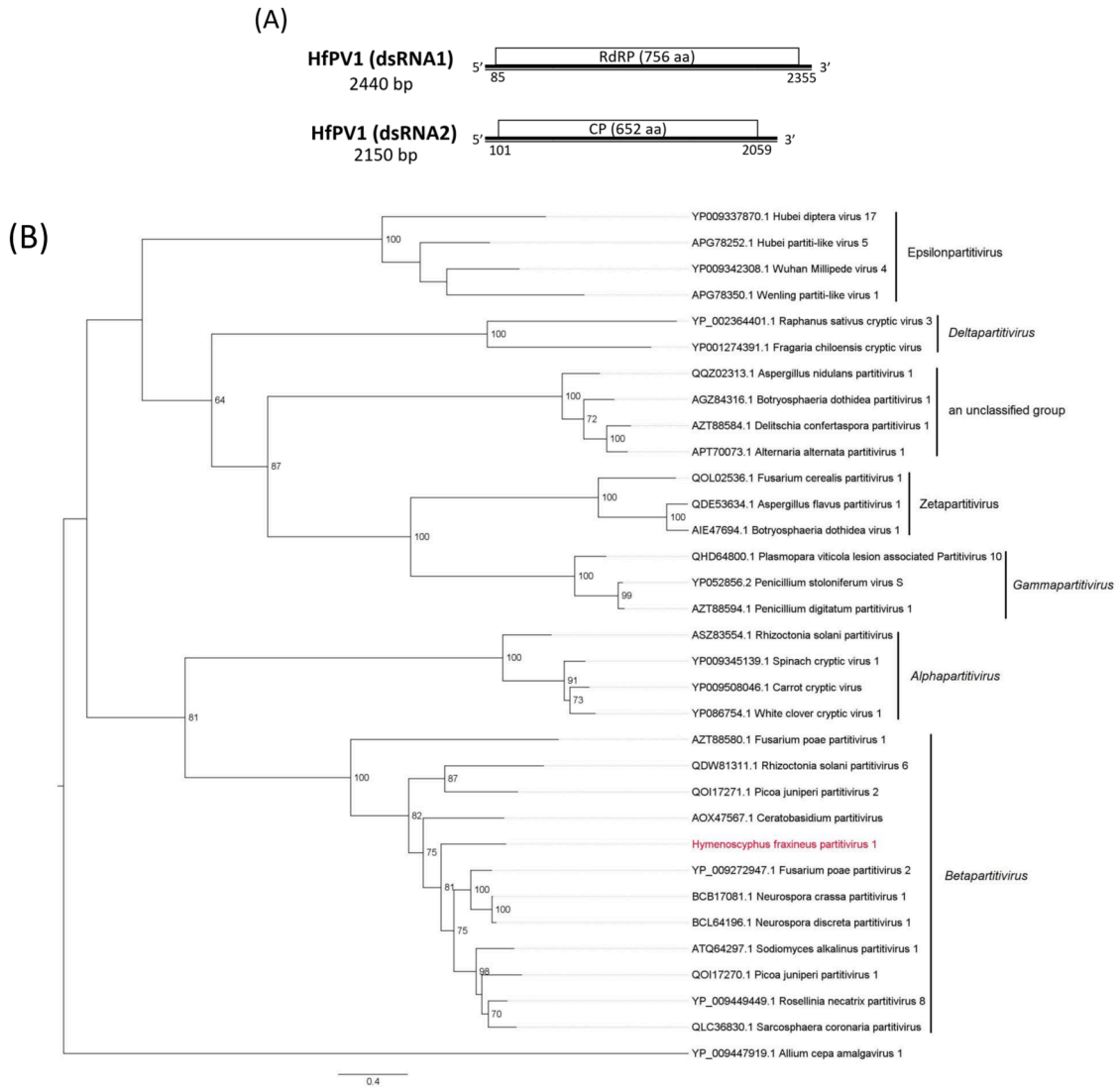

Fig. 5. (A) Genomic organization of the HfPV1 with a bi-segmented dsRNA. The positive strand of the dsRNA1 encodes for RdRP and includes a 84-nt 5′ UTR, an ORF1 encoding 756 aa protein and a 85-nt 3′ UTR. The dsRNA2 encodes for CP and includes a 100-nt 5′ UTR, an ORF encoding 652 aa protein and 91-nt 3′ UTR. (B) Phylogenetic analysis of HfPV1. Maximum-likelihood tree based on RNA-dependent RNA polymerase of HfPV1. Numbers at nodes are bootstrap values out of 1000 replicates. Allium cepa amalgavirus 1 is used as an outgroup to root the tree. Bootstrap values (%) less than 60 are not shown.

HfNSRV1 and other (–)ssRNA viruses revealed that HfNSRV1 grouped with viruses infecting fungi and other hosts forming a distinct clade in the proposed family "Mybuviridae" (Ruiz-Padilla et al., 2021) (Fig. 6B). The species demarcation criteria have currently not been defined for mybuviruses, however, our data suggested that the virus might belong to a new species. The virus was tentatively named Hymenoscyphus fraxineus negative stranded RNA virus 1 (HfNSRV1).

4. Discussion

4.1. Virus prevalence and diversity in Hymenoscyphus fraxineus

Mycoviruses are widespread in all major groups of fungi and are generally associated with a latent infection of their host (Ghabrial and Suzuki, 2009). In regard to plant pathogenic fungi, of particular interest are mycoviruses causing debilitating diseases and/or reducing the virulence of their host, as they may represent potential biological control agents for the fungal pathogen (Rigling et al., 2021). In the present study, we used a HTS approach to assess the prevalence and diversity of RNA viruses in two Japanese populations of *H. fraxineus*, the causal agent of ash dieback is Europe. Since the fungus is native to East Asia (Gross et al., 2014b), possible biological control agents are more likely to be found in populations from that part of the world. In the invasive European population of *H. fraxineus*, a mycovirus (HfMV1) was previously detected (Čermáková et al., 2017; Schoebel et al., 2017, 2014), but its high prevalence in Europe (28 to 90%) suggests it does not significantly affect pathogen virulence.

Both Japanese populations of *H. fraxineus* show a low prevalence (overall 11.2% virus-infected isolates), but a high diversity in viruses with five different RNA virus groups. Mycovirus prevalence in fungal populations varies considerably among fungal species. For example, Arjona-Lopez et al. (2018) found only 14% of Mediterranean isolates of the plant pathogenic ascomycete *Rosellinia necatrix* to be virus-infected. On the other hand, Mu et al. (2017) identified 57 mycoviruses in 85 Australian isolates of *Sclerotinia sclerotiorum*, whereas Ruiz-Padilla et al. (2021) detected 92 mycoviruses in a collection of 248 isolates of the necrotrophic fungus *Botrytis cinerea*.

All five *H. fraxineus* viruses detected in this study are novel members within three established families (*Mito-, Partiti-* and *Endornaviridae*), one established genus (*Botybirnavirus*) and one previously proposed family ("Mybuviridae"), and were detected for the first time in *H. fraxineus*. Compared to other plant pathogenic fungi, virus diversity in this fungal

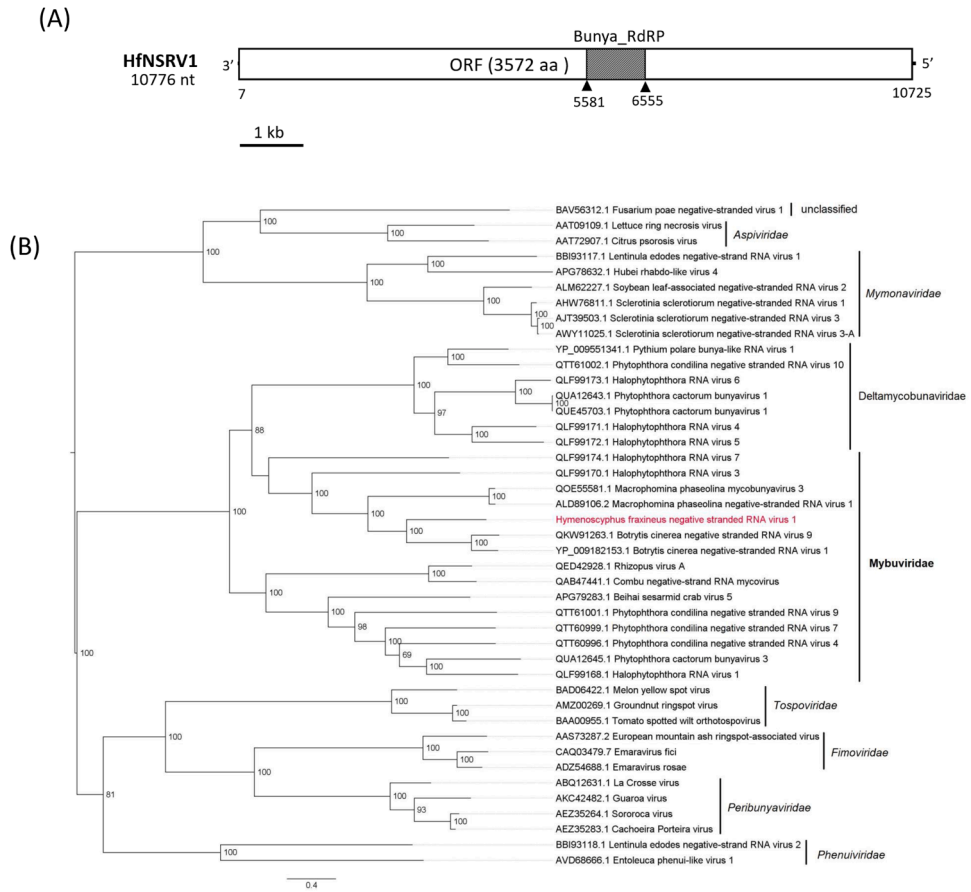

Fig. 6. (A) Schematic representation of the HfNSRV1 showing the ORF and the conserved domain for Bunya_RdRP at nt position 5581–6555. (B) Phylogenetic analysis of HfNSRV1. Maximum-likelihood tree was generated based on the amino acid alignment of the deduced ORF (L protein polymerases). Numbers at nodes are bootstrap values out of 1000 replicates. Bootstrap values (%) less than 60 are not shown.

species is rather low, since there are studies describing RNA viruses from 10 to 21 groups or families in single fungal species (Arjona-Lopez et al., 2018; Chiba et al., 2013, 2016, 2009; Mu et al., 2017). Nevertheless, it should be noticed that 13 *H. fraxineus* isolates were virus-infected in our study and some of the newly reported mycoviruses present special features as mentioned below. Additionally, the RNA-seq pools included quite many RNA samples (24 to 31 samples in each analysis) and in BLASTx (but BLASTn) only contigs of >1000 nt were used for queries of analyses. Thus, small contigs of low titre viruses may have been missed during analyses. Noteworthy, the mitovirus HfMV1, which is widespread in the European population of *H. fraxineus,* was not found in the two Japanese populations of the fungus. This could suggest that the *H. fraxineus* strains introduced into Europe did not originate from Japan, but from other areas within the native range of the fungus in East Asia. Alternatively, HfMV1 may be rare in Japan and, thus, additional populations should be screened to detect it. In this case, the high prevalence of HfMV1 in the European population may be due to a founder effect.

4.2. A second *Hymenoscyphus fraxineus* mitovirus with a unique genomic form

A novel mitovirus (HfMV2), a member of the family *Mitoviridae*, was detected in 7.8% of the screened Japanese isolates of *H. fraxineus*. Although HfMV2 was found in both populations, most variants were detected only in Hokkaido. This might be due to the larger sample size of this population compared to the population of Sugadaira. Our analyses suggest that the RNA genome of HfMV2 has two forms, i.e. linear and circular. Some RNA mycoviruses (including mitoviruses) were proposed to have a circular genome nature, but experimental evidence provided was not enough to support this hypothesis (Hintz et al., 2013; Lakshman et al., 1998), except for a few reports, such as the existence of a circular RNA replicon in yeast 20S RNA (Matsumoto et al., 1990) and the recently reported Sclerotinia sclerotiorum yadokarivirus 1 (Jia et al., 2022). Circular RNAs (circRNAs) have also been reported in human and animal RNA viruses where they have established a new class of non-coding RNAs (Pan et al., 2021; Yao et al., 2021). In animals, the circRNAs are known as microRNA sponges, regulating microRNAs. They also play a role in protein sequestration, transcription regulation and potential function in cancer (Cortés-López and Miura, 2016). The circular genomic form confers resistance against the exonucleases, thus circular RNA viruses are more stable compared to linear RNAs (Zhang et al., 2016b).

HfMV2 shares over 35% amino acid sequence identity to OnuMV7, a virus in the genus *Kvaramitovirus* identified in the ascomycete *Ophiostoma novo-ulmi*, one of the two causal agents of Dutch elm disease (Hintz et al., 2013). Interestingly, the mitovirus HfMV1 found in the European population of *H. fraxineus* (Čermáková et al., 2017; Schoebel et al., 2017, 2014) belongs to the genus *Unuamitovirus* (Fig. 1B) and is not closely related to HfMV2 (~30% identity between the two at aa level). The apparently unrelatedness of HfMV2 with HfMV1 and its resemblance to OnuMV7 in the phylogenetic analysis, suggests that HfMV2 might have originated from the same ancestor as the Dutch elm mitovirus (OnuMV7). Dutch elm disease is reported to occur on the island of Hokkaido (Masuya et al., 2010), from where one of the two *H. fraxineus* populations analysed in this study originates. To better understand the origin of HfMV2 it would be of great interest to screen populations of fungi, including *O. novo-ulmi,* from Hokkaido for the presence of similar viruses. Horizontal viral transmission via hyphal anastomosis usually

occurs between vegetatively compatible fungal individuals of the same species (Rosewich and Kistler, 2000). However, Ophiostoma mitovirus 3b found in *O. novo ulmi* is conspecific with a virus in *Botrytis cinerea* (Wu et al., 2010) and a dsRNA virus conferring hypovirulence in *Sclerotinia homoeocarpa* is conspecific with Ophiostoma mitovirus 3a-Ld (Deng et al., 2003). The presence of the same mitovirus in different groups of fungi may indicate a horizontal virus transfer between fungal species, as previously suggested by Arjona-Lopez et al. (2018). Alternative to hyphal anastomosis, Yaegashi et al. (2013) hypothesized the presence of an undefined vector organism facilitating the transfer of viruses between fungal groups. The host range of HfMV2 may also be investigated by using protoplast fusion, an artificial introduction method already applied, for example, to Cyrphonectria parasitica mitovirus 1 (Shahi et al., 2019).

4.3. A new endornavirus with an accessory helicase

One of the Japanese isolates screened showed a co-infection by HfMV2 and a novel endornavirus (HfEV1). Co-infection of a single fungal isolate by two or more viruses is a common phenomenon and can result in a complex interplay between viruses, with effects on the host different than in single infections (Sasaki et al., 2016; Sun et al., 2006; Yang et al., 2021). Endornaviruses encode a single large polypeptide including different conserved domains (Fukuhara and Gibbs, 2012; Valverde et al., 2019). The RdRP domain is ubiquitous to all endornaviruses, but the composition of the other domains is highly variable. Song et al. (2013) hypothesized that such domains might have originated from other organisms as a result of horizontal gene transfer (HGT) with some independent events. HGT enables the exchange of genetic material between distantly related organisms and plays a significant role in evolution (Gogarten and Townsend, 2005). However, even though HGT is common to archaea, bacteria and viruses, its relevance in eukaryotes is controversial (Alexander et al., 2016).

HfEV1 shares over 48% sequence identity, as well as most genomic features, including the presence of CRR, an MTR domain and two helicase domains (DExH and Hel), with Sclerotinia sclerotiorum endornaviruses. A Phytoreo_S7 domain (involved in putative nucleic acid binding) is absent in HfEV1 (Fig. 3A). Helicases are essential enzymes involved in all aspects of nucleic acid metabolism, including replication, repair, and recombination, and are classified into six superfamilies based on the conserved motifs and functional analysis (Singleton et al., 2007). Apart in some endornaviruses (Tuomivirta et al., 2009), the presence of two helicase domains has been predicted in other groups of (+)ssRNA mycoviruses, like tymo-like viruses (Koonin et al., 1993), fusariviruses (Abdoulaye et al., 2022), and hypoviruses (Abdoulaye et al., 2021). The accessory helicase of Rhizoctonia solani fusarivirus 4 (RsFV4) was considered an evolutionary link between fusari-, hypo- and plant potyviruses (Abdoulaye et al., 2022). A phylogenetic analysis of the DExH/HrpA domain encoded by HfEV1 and related betaendornaviruses revealed a shared ancestry with animal pestiviruses ((+)ssRNA viruses in the family *Flaviviridae* (Fig. S5b)). This result suggests that the DExH/HrpA domain in HfEV1 might have originated through HGT event (s) with ancestral RNA viruses related to animal viruses. However, scientific evidence about the relationship between mycoviruses and animal viruses is still lacking.

4.4. Novel double stranded RNA viruses in the Japanese population

Two novel dsRNA viruses were also identified in the present study. The botybirnavirus (HfBRV1) had the properties characteristic of the genus *Botybirnavirus,* including 1) a bi-segmented dsRNA genome, 2) a single large ORF encoded by each of the dsRNA segments, and 3) long conserved 5′ UTRs between the two segments. The presence of an alignable region between the two ORF proteins of HfBRV1 also supports it to be a member of the genus *Botybirnavirus* (see results). Such regions have been reported in other botybirnaviruses (SsBRV1, Bipolaris maydis botybirnavirus 1, Alternaria alternata botybirnavirus 1), indicating a potential duplicated region of the structural proteins (Liu et al., 2015; Shamsi et al., 2019; Wang et al., 2018).

A number of dsRNA and (+)ssRNA mycoviruses exhibit internal ribosome entry site (IRES) activities in their long 5′-UTRs (Chiba et al., 2018). The usual signature sequence for IRES is the presence of multiple AUGs in the 5′-UTR. Each of the dsRNA 1 and 2 of HfBRV1 have 5′ AUGs upstream of the authentic ORF start codon. The HfBRV1 5′-UTRs have predicted the presence of a potential IRES with the online IRESPred program (http://bioinfo.unipune.ac.in/IRESPred/home.html) (W. Shamsi and Prospero S., unpublished results). Biochemical analyses (e.g., single and dual luciferase assay systems (Chiba et al., 2018)) would be required to confirm their IRES activities.

The second dsRNA virus was a partitivirus (HfPV1) that belongs to the genus *Betapartitivirus*. The HfPV1 was found to have an additional putative CP-like segment (see results). Some tri-segmented partitiviruses (deltapartitiviruses) have been reported to have different variants of dsRNA2 encoding for variable, but related versions of the CP (Nibert et al., 2014). In other partitiviruses (gammapartitiviruses), the third dsRNA segment encodes a hypothetical protein with unknown function (s) (Liu et al., 2008; Tuomivirta and Hantula, 2005; Zhang et al., 2013). Based on the alignment of the HfPV1 contig sequences (supplementary file 7), the two CP-like segments likely share the terminal sequences. Therefore, we assume that the virus has two CP variants, although the sequencing of internal and termini together with the biochemical analysis of its virions is needed to confirm this finding.

4.5. A novel negative-stranded RNA virus with a potential to form segmented genome

A novel (–)ssRNA virus (HfNSRV1) was also identified in the Japanese *H. fraxineus* isolates. The discovery rate of (–)ssRNA virus is still low in fungi. HfNSRV1 has a long RNA segment and the encoded protein contains a Bunya-RdRP domain. The order *Bunyavirales* includes many segmented (–)ssRNA viruses infecting animals and plants (Maes et al., 2018). Sequence analysis of the L protein confirmed the relatedness between HfNSRV1 and other known segmented (–)ssRNA viruses. First, a conserved "SDD" tri-peptide sequence is present in the motif C (Fig. S9a), as observed in the majority of segmented (–)ssRNA viruses. Second, segmented (–)ssRNA viruses (including phenuiviruses) possess the N-termini endonuclease domain with an endonuclease activity. Alignment of the N-termini regions revealed the presence of a putative endonuclease domain in HfNSRV1 L protein. The endonuclease domain contains the key residues (*H* + PD and D/ExK motifs) that are involved in cation-dependent nucleases (Fig. S9b). The endonuclease activity is required for the "cap-snatching" mechanism where the host mRNA is cleaved by the viral polymerase, and the capped fragment is employed for viral transcription (Holm et al., 2018; Sun et al., 2018).

Replication of (–)ssRNA viruses seems to require the ribonucleoprotein complex, which is associated with the viral nucleoprotein (NC) (Sun et al., 2018). Therefore, (–)ssRNA viruses in the order *Bunyavirales* might have multiple RNA segments encoding at least the NC gene (Lin et al., 2019). Such additional segment(s), however, were not identified in HfNSRV1 in the current study. Thus, further investigation would be needed to uncover the entire genome structure of HfNSRV1.

4.6. Mycovirus-mediated control of ash dieback?

In this study, we were able to detect and characterize five new RNA mycoviruses in Japanese populations of *H. fraxineus*, the causal agent of ash dieback in Europe. Since, to date, no effective control method is available for this invasive disease, such parasitic mycoviruses may provide the basis for virus-mediated control of ash dieback. However, for a virus to act as a biological control agent of its fungal host, four criteria must be fulfilled (Rigling et al., 2021), i.e. (i) it must reduce the virulence of the pathogen, (ii) it must be transmissible to virus-free

strains of the pathogen, (iii) it must be able to overcome the cellular defence mechanisms of the fungal host, and (iv) it must be able to replicate and spread through the fungal mycelia. Hence, upcoming investigations will test the detected mycoviruses for these basic properties.

Declaration of Competing Interest

The authors declare that they have no known competing financial interests or personal relationships that could have appeared to influence the work reported in this paper.

Data availability

Data will be made available on request.

Acknowledgments

This study was conducted in the frame of the HOMED project (http://homed-project.eu/), which received funding from the European Union's Horizon 2020 Research and Innovation Program under grant agreement No. 771271. SP also received financial support by two grants (gSO H. fra / B156B0625 and 00.5053.PZ / A073D1BAD) from the Swiss Federal Office for the Environment FOEN. We thank the three reviewers and the editor for the valuable comments on a previous version of the manuscript.

Supplementary materials

Supplementary material associated with this article can be found, in the online version, at doi:10.1016/j.virusres.2022.198901.

References

Abdoulaye, A.H., Hai, D., Tang, Q., Jiang, D., Fu, Y., Cheng, J., Lin, Y., Li, B., Kotta-Loizou, I., Xie, J., 2021. Two distant helicases in one mycovirus: evidence of horizontal gene transfer between mycoviruses, coronaviruses and other nidoviruses. Virus Evol. 7 (1), veab043.

Abdoulaye, A.H., Jia, J., Abbas, A., Hai, D., Cheng, J., Fu, Y., Lin, Y., Jiang, D., Xie, J., 2022. Fusarivirus accessory helicases present an evolutionary link for viruses infecting plants and fungi. Virol. Sin. 37 (3), 427–436. https://doi.org/10.1016/j.virs.2022.03.010.

Alexander, W.G., Wisecaver, J.H., Rokas, A., Hittinger, C.T., 2016. Horizontally acquired genes in early-diverging pathogenic fungi enable the use of host nucleosides and nucleotides. Proc. Natl. Acad. Sci. U. S. A. 113 (15), 4116–4121.

Andika, I.B., Wei, S., Cao, C., Salaipeth, L., Kondo, H., Sun, L., 2017. Phytopathogenic fungus hosts a plant virus: a naturally occurring cross-kingdom viral infection. Proc. Natl. Acad. Sci. U. S. A. 114 (46), 12267–12272.

Arjona-Lopez, J.M., Telengech, P., Jamal, A., Hisano, S., Kondo, H., Yelin, M.D., Arjona-Girona, I., Kanematsu, S., Lopez-Herrera, C.J., Suzuki, N., 2018. Novel, diverse RNA viruses from Mediterranean isolates of the phytopathogenic fungus, *Rosellinia necatrix*: insights into evolutionary biology of fungal viruses. Environ. Microbiol. 20 (4), 1464–1483.

Bartholomäus, A., Wibberg, D., Winkler, A., Pühler, A., Schlüter, A., Varrelmann, M., 2016. Deep sequencing analysis reveals the mycoviral diversity of the virome of an avirulent isolate of *Rhizoctonia solani* AG-2-2 IV. PLoS One 11 (11), e0165965.

Botella, L., Janoušek, J., Maia, C., Jung, M.H., Raco, M., Jung, T., 2020. Marine oomycetes of the genus *Halophytophthora* harbor viruses related to bunyaviruses. Front. Microbiol. 11, 1467.

Čermáková, V., Eichmeier, A., Herrero, N., Botella, L., 2017. HfMV 1 and another putative mycovirus in central european populations of *Hymenoscyphus fraxineus*, the causal agent of ash dieback in Europe. Balt. For. 23 (1), 107–115.

Chiba, S., Jamal, A., Suzuki, N., 2018. First evidence for internal ribosomal entry sites in diverse fungal virus genomes. mBio 9 (2), e02350.

Chiba, S., Lin, Y.H., Kondo, H., Kanematsu, S., Suzuki, N., 2013. A novel victorivirus from a phytopathogenic fungus, *Rosellinia necatrix*, is infectious as particles and targeted by RNA silencing. J. Virol. 87 (12), 6727–6738.

Chiba, S., Lin, Y.H., Kondo, H., Kanematsu, S., Suzuki, N., 2016. A novel betapartitivirus RnPV6 from *Rosellinia necatrix* tolerates host RNA silencing but is interfered by its defective RNAs. Virus Res. 219, 62–72.

Chiba, S., Salaipeth, L., Lin, Y.H., Sasaki, A., Kanematsu, S., Suzuki, N., 2009. A novel bipartite double-stranded RNA mycovirus from the white root rot fungus *Rosellinia necatrix*: molecular and biological characterization, taxonomic considerations, and potential for biological control. J. Virol. 83 (24), 12801–12812.

Choi, G.H., Nuss, D.L., 1992. Hypovirulence of chestnut blight fungus conferred by an infectious viral cDNA. Science 257 (5071), 800–803.

Cortés-López, M., Miura, P., 2016. Focus: epigenetics: emerging functions of circular RNAs. Yale J. Biol. Med. 89 (4), 527.

Deng, F., Xu, R., Boland, G.J., 2003. Hypovirulence-associated double-stranded RNA from *Sclerotinia homoeocarpa* is conspecific with Ophiostoma novo-ulmi mitovirus 3a-Ld. Phytopathology 93 (11), 1407–1414.

Donaire, L., Ayllón, M.A., 2017. Deep sequencing of mycovirus-derived small RNAs from *Botrytis* species. Mol. Plant Pathol. 18 (8), 1127–1137.

Donaire, L., Pagán, I., Ayllón, M.A., 2016. Characterization of *Botrytis cinerea* negative-stranded RNA virus 1, a new mycovirus related to plant viruses, and a reconstruction of host pattern evolution in negative-sense ssRNA viruses. Virology 499, 212–218.

Enderle, R., Sander, F., Metzler, B., 2017. Temporal development of collar necroses and butt rot in association with ash dieback. iFor Biogeosci. For. 10 (3), 529.

Eusebio-Cope, A., Suzuki, N., 2015. Mycoreovirus genome rearrangements associated with RNA silencing deficiency. Nucleic Acids. Res. 43 (7), 3802–3813.

Fukuhara, T., Gibbs, M.J., 2012. Family *Endornaviridae*. Virus Taxon. Ninth Rep. Int. Comm. Taxon. Viruses 519–521.

Ghabrial, S.A., Castón, J.R., Jiang, D., Nibert, M.L., Suzuki, N., 2015. 50-plus years of fungal viruses. Virology 479-480, 356–368.

Ghabrial, S.A., Suzuki, N., 2009. Viruses of plant pathogenic fungi. Annu. Rev. Phytopathol. 47, 353–384.

Gogarten, J.P., Townsend, J.P., 2005. Horizontal gene transfer, genome innovation and evolution. Nat. Rev. Microbiol. 3 (9), 679–687.

Gross, A., Holdenrieder, O., Pautasso, M., Queloz, V., Sieber, T.N., 2014a. *Hymenoscyphus fraxineus*, the causal agent of European ash dieback. Mol. Plant Pathol. 15 (1), 5–21.

Gross, A., Hosoya, T., Queloz, V., 2014b. Population structure of the invasive forest pathogen *Hymenoscyphus fraxineus*. Mol. Ecol. 23 (12), 2943–2960.

Guindon, S., Dufayard, J.F., Lefort, V., Anisimova, M., Hordijk, W., Gascuel, O., 2010. New algorithms and methods to estimate maximum-likelihood phylogenies: assessing the performance of PhyML 3.0. Syst. Biol. 59 (3), 307–321.

Halecker, S., Wennrich, J.P., Rodrigo, S., Andrée, N., Rabsch, L., Baschien, C., Steinert, M., Stadler, M., Surup, F., Schulz, B., 2020. Fungal endophytes for biocontrol of ash dieback: the antagonistic potential of *Hypoxylon rubiginosum*. Fungal Ecol. 45, 100918.

Heinze, C., 2012. A novel mycovirus from *Clitocybe odora*. Arch. Virol. 157 (9), 1831–1834.

Hillman, B.I., Annisa, A., Suzuki, N., 2018. Viruses of plant-interacting fungi. Adv. Virus Res. 100, 99–116.

Hintz, W.E., Carneiro, J.S., Kassatenko, I., Varga, A., James, D., 2013. Two novel mitoviruses from a Canadian isolate of the Dutch elm pathogen *Ophiostoma novo-ulmi* (93–1224). Virol. J. 10 (1), 252.

Hollings, M., 1962. Viruses associated with a die-back disease of cultivated mushroom. Nature 196, 962.

Holm, T., Kopicki, J.D., Busch, C., Olschewski, S., Rosenthal, M., Uetrecht, C., Günther, S., Reindl, S., 2018. Biochemical and structural studies reveal differences and commonalities among cap-snatching endonucleases from segmented negative-strand RNA viruses. J. Biol. Chem. 293 (51), 19686–19698.

Jamal, A., Sato, Y., Shahi, S., Shamsi, W., Kondo, H., Suzuki, N., 2019. Novel victorivirus from a Pakistani isolate of *Alternaria alternata* lacking a typical translational stop/restart sequence signature. Viruses 11 (6), 577. https://doi.org/10.3390/v11060577.

Jia, J., Mu, F., Fu, Y., Cheng, J., Lin, Y., Li, B., Jiang, D., Xie, J., Simon Anne, E., 2022. A capsidless virus is trans-encapsidated by a bisegmented botybirnavirus. J. Virol. 0 (0), e00296.

Katoh, K., Toh, H., 2008. Recent developments in the MAFFT multiple sequence alignment program. Brief. Bioinform. 9 (4), 286–298.

Kondo, H., Botella, L., Suzuki, N., 2022. Mycovirus diversity and evolution revealed/inferred from recent studies. Annu. Rev. Phytopathol.

Koonin, E.V., Dolja, V.V., Krupovic, M., 2015. Origins and evolution of viruses of eukaryotes: the ultimate modularity. Virology 479-480, 2–25.

Koonin, E.V., Dolja, V.V., Morris, T.J., 1993. Evolution and taxonomy of positive-strand RNA viruses: implications of comparative analysis of amino acid sequences. Crit. Rev. Biochem. Mol. Biol. 28 (5), 375–430.

Kosawang, C., Amby, D.B., Bussaban, B., McKinney, L.V., Xu, J., Kjær, E.D., Collinge, D. B., Nielsen, L.R., 2018. Fungal communities associated with species of *Fraxinus* tolerant to ash dieback, and their potential for biological control. Fungal Biol. 122 (2–3), 110–120.

Kotta-Loizou, I., Coutts, R.H.A., Ictv Report, C., 2022. ICTV virus taxonomy profile: *Polymycoviridae* 2022. J. Gen. Virol. 103 (5).

Kowalski, T., Holdenrieder, O., 2009. The teleomorph of *Chalara fraxinea*, the causal agent of ash dieback. For. Pathol. 39 (5), 304–308.

Lakshman, D.K., Jian, J., Tavantzis, S.M., 1998. A double-stranded RNA element from a hypovirulent strain of *Rhizoctonia solani* occurs in DNA form and is genetically related to the pentafunctional AROM protein of the shikimate pathway. Proc. Natl. Acad. Sci. U. S. A. 95 (11), 6425–6429.

Lin, Y.H., Fujita, M., Chiba, S., Hyodo, K., Andika, I.B., Suzuki, N., Kondo, H., 2019. Two novel fungal negative-strand RNA viruses related to *Mymonaviruses* and *Phenuiviruses* in the shiitake mushroom (*Lentinula edodes*). Virology 533, 125–136.

Liu, H., Fu, Y., Jiang, D., Li, G., Xie, J., Peng, Y., Yi, X., Ghabrial, S.A., 2009. A novel mycovirus that is related to the human pathogen hepatitis E virus and rubi-like viruses. J. Virol. 83 (4), 1981–1991.

Liu, L., Wang, Q., Cheng, J., Fu, Y., Jiang, D., Xie, J., 2015. Molecular characterization of a bipartite double-stranded RNA virus and its satellite-like RNA co-infecting the phytopathogenic fungus *Sclerotinia sclerotiorum*. Front. Microbiol. 6, 406.

Liu, L., Xie, J., Cheng, J., Fu, Y., Li, G., Yi, X., Jiang, D., 2014. Fungal negative-stranded RNA virus that is related to *Bornaviruses* and *Nyaviruses*. Proc. Natl. Acad. Sci. U. S. A. 111 (33), 12205–12210.

Liu, W., Duns, G., Chen, J., 2008. Genomic characterization of a novel partitivirus infecting. *Aspergillus ochraceus*. Virus Genes 37 (3), 322–327.
Lygis, V., Prospero, S., Burokiene, D., Schoebel, C.N., Marciulyniene, D., Norkute, G., Rigling, D., 2017. Virulence of the invasive ash pathogen *Hymenoscyphus fraxineus* in old and recently established populations. Plant Pathol. 66 (5), 783–791.
Maes, P., Alkhovsky, S.V., Bào, Y., Beer, M., Birkhead, M., Briese, T., Buchmeier, M.J., Calisher, C.H., Charrel, R.N., Choi, I.R., Clegg, C.S., de la Torre, J.C., Delwart, E., DeRisi, J.L., Di Bello, P.L., Di Serio, F., Digiaro, M., Dolja, V.V., Drosten, C., Druciarek, T.Z., Du, J., Ebihara, H., Elbeaino, T., Gergerich, R.C., Gillis, A.N., Gonzalez, J.P.J., Haenni, A.L., Hepojoki, J., Hetzel, U., Hồ, T., Hóng, N., Jain, R.K., Jansen van Vuren, P., Jin, Q., Jonson, M.G., Junglen, S., Keller, K.E., Kemp, A., Kipar, A., Kondov, N.O., Koonin, E.V., Kormelink, R., Korzyukov, Y., Krupovic, M., Lambert, A.J., Laney, A.G., LeBreton, M., Lukashevich, I.S., Marklewitz, M., Markotter, W., Martelli, G.P., Martin, R.R., Mielke-Ehret, N., Mühlbach, H.P., Navarro, B., Ng, T.F.F., Nunes, M.R.T., Palacios, G., Pawęska, J.T., Peters, C.J., Plyusnin, A., Radoshitzky, S.R., Romanowski, V., Salmenperä, P., Salvato, M.S., Sanfaçon, H., Sasaya, T., Schmaljohn, C., Schneider, B.S., Shirako, Y., Siddell, S., Sironen, T.A., Stenglein, M.D., Storm, N., Sudini, H., Tesh, R.B., Tzanetakis, I.E., Uppala, M., Vapalahti, O., Vasilakis, N., Walker, P.J., Wáng, G., Wáng, L., Wáng, Y., Wèi, T., Wiley, M.R., Wolf, Y.I., Wolfe, N.D., Wú, Z., Xú, W., Yang, L., Yāng, Z., Yeh, S.D., Zhāng, Y.Z., Zhèng, Y., Zhou, X., Zhū, C., Zirkel, F., Kuhn, J.H., 2018. Taxonomy of the family *Arenaviridae* and the order *Bunyavirales*: update 2018. Arch. Virol. 163 (8), 2295–2310.
Marchler-Bauer, A., Bo, Y., Han, L., He, J., Lanczycki, C.J., Lu, S., Chitsaz, F., Derbyshire, M.K., Geer, R.C., Gonzales, N.R., Gwadz, M., Hurwitz, D.I., Lu, F., Marchler, G.H., Song, J.S., Thanki, N., Wang, Z., Yamashita, R.A., Zhang, D., Zheng, C., Geer, L.Y., Bryant, S.H., 2016. CDD/SPARCLE: functional classification of proteins via subfamily domain architectures. Nucleic Acids Res. 45 (D1), D200–D203.
Marzano, S.L., Nelson, B.D., Ajayi-Oyetunde, O., Bradley, C.A., Hughes, T.J., Hartman, G. L., Eastburn, D.M., Domier, L.L., 2016. Identification of diverse mycoviruses through metatranscriptomics characterization of the viromes of five major fungal plant pathogens. J. Virol. 90 (15), 6846–6863.
Masuya, H., Brasier, C., Ichihara, Y., Kubono, T., Kanzaki, N., 2010. First report of the Dutch elm disease pathogens *Ophiostoma ulmi* and *O. novo-ulmi* in Japan. Plant Pathol. 59 (4), 805. -805.
Mathews, D.H., Disney, M.D., Childs, J.L., Schroeder, S.J., Zuker, M., Turner, D.H., 2004. Incorporating chemical modification constraints into a dynamic programming algorithm for prediction of RNA secondary structure. Proc. Natl. Acad. Sci. U. S. A. 101 (19), 7287–7292.
Matsumoto, Y., Fishel, R., Wickner, R.B., 1990. Circular single-stranded RNA replicon in *Saccharomyces cerevisiae*. Proc. Natl. Acad. Sci. U. S. A. 87 (19), 7628–7632.
McKinney, L.V., Nielsen, L.R., Collinge, D.B., Thomsen, I.M., Hansen, J.K., Kjær, E.D., 2014. The ash dieback crisis: genetic variation in resistance can prove a long-term solution. Plant Pathol. 63 (3), 485–499.
McKinney, L.V., Nielsen, L.R., Hansen, J.K., Kjær, E.D., 2011. Presence of natural genetic resistance in *Fraxinus excelsior* (Oleraceae) to *Chalara fraxinea* (Ascomycota): an emerging infectious disease. Heredity 106 (5), 788–797 (Edinb).
McMullan, M., Rafiqi, M., Kaithakottil, G., Clavijo, B.J., Bilham, L., Orton, E., Percival-Alwyn, L., Ward, B.J., Edwards, A., Saunders, D.G.O., Garcia Accinelli, G., Wright, J., Verweij, W., Koutsovoulos, G., Yoshida, K., Hosoya, T., Williamson, L., Jennings, P., Ioos, R., Husson, C., Hietala, A.M., Vivian-Smith, A., Solheim, H., MaClean, D., Fosker, C., Hall, N., Brown, J.K.M., Swarbreck, D., Blaxter, M., Downie, J.A., Clark, M.D., 2018. The ash dieback invasion of Europe was founded by two genetically divergent individuals. Nat. Ecol. Evol. 2 (6), 1000–1008.
Mu, F., Xie, J., Cheng, S., You, M.P., Barbetti, M.J., Jia, J., Wang, Q., Cheng, J., Fu, Y., Chen, T., Jiang, D., 2017. Virome characterization of a collection of *S. sclerotiorum* from Australia. Front Microbiol. 8, 2540.
Nibert, M.L., Ghabrial, S.A., Maiss, E., Lesker, T., Vainio, E.J., Jiang, D., Suzuki, N., 2014. Taxonomic reorganization of family *Partitiviridae* and other recent progress in partitivirus research. Virus Res. 188, 128–141.
Osaki, H., Sasaki, A., Nomiyama, K., Tomioka, K., 2016. Multiple virus infection in a single strain of *Fusarium poae* shown by deep sequencing. Virus Genes 52 (6), 835–847.
Pan, J., Zhang, X., Zhang, Y., Yan, B., Dai, K., Zhu, M., Liang, Z., Dai, Y., Zhang, M., Zhang, Z., Zhu, H., Gu, Y., Cao, M., Xue, R., Cao, G., Hu, X., Gong, C., 2021. Grass carp reovirus encoding circular RNAs with antiviral activity. Aquaculture 533, 736135.
Prospero, S., Botella, L., Santini, A., Robin, C., 2021. Biological control of emerging forest diseases: how can we move from dreams to reality? For. Ecol. Manag. 496, 119377.
Prospero, S., Rigling, D., 2016. Using molecular markers to assess the establishment and spread of a mycovirus applied as a biological control agent against chestnut blight. BioControl 61 (3), 313–323.
Rigling, D., Prospero, S., 2018. *Cryphonectria parasitica*, the causal agent of chestnut blight: invasion history, population biology and disease control. Mol. Plant Pathol. 19 (1), 7–20.
Rigling, D., Robin, C., Prospero, S., 2021. Mycovirus-mediated biological control. In: Bamford, D.H., Zuckerman, M. (Eds.), Encyclopedia of Virology, 4th ed. Academic Press, Oxford, pp. 468–477.
Rosewich, U.L., Kistler, H.C., 2000. Role of horizontal gene transfer in the evolution of fungi. Annu. Rev. Phytopathol. 38, 325–363.
Ruiz-Padilla, A., Rodríguez-Romero, J., Gómez-Cid, I., Pacifico, D., Ayllón, M.A., Wickner, R.B., 2021. Novel mycoviruses discovered in the mycovirome of a necrotrophic fungus. mBio 12 (3), e03705–e03720.
Sasaki, A., Nakamura, H., Suzuki, N., Kanematsu, S., 2016. Characterization of a new megabirnavirus that confers hypovirulence with the aid of a co-infecting partitivirus to the host fungus, *Rosellinia necatrix*. Virus Res. 219, 73–82.
Sato, Y., Shamsi, W., Jamal, A., Bhatti, M.F., Kondo, H., Suzuki, N., Wickner, R.B., 2020. Hadaka virus 1: a capsidless eleven-segmented positive-sense single-stranded RNA Virus from a phytopathogenic fungus, *Fusarium oxysporum*. mBio 11 (3), e00450.
Schlegel, M., Dubach, V., von Buol, L., Sieber, T.N., 2016. Effects of endophytic fungi on the ash dieback pathogen. FEMS Microbiol. Ecol. 92 (9), fiw142 https://doi.org/10.1093/femsec/fiw142.
Schoebel, C.N., Botella, L., Lygis, V., Rigling, D., 2017. Population genetic analysis of a parasitic mycovirus to infer the invasion history of its fungal host. Mol. Ecol. 26 (9), 2482–2497.
Schoebel, C.N., Zoller, S., Rigling, D., 2014. Detection and genetic characterisation of a novel mycovirus in *Hymenoscyphus fraxineus*, the causal agent of ash dieback. Infect. Genet. Evol. 28, 78–86.
Shahi, S., Eusebio-Cope, A., Kondo, H., Hillman, B.I., Suzuki, N., Simon, A.E., 2019. Investigation of host range of and host defense against a mitochondrially replicating mitovirus. J. Virol. 93 (6), e01503–e01518.
Shamsi, W., Sato, Y., Jamal, A., Shahi, S., Kondo, H., Suzuki, N., Bhatti, M.F., 2019. Molecular and biological characterization of a novel botybirnavirus identified from a Pakistani isolate of *Alternaria alternata*. Virus Res. 263, 119–128.
Singleton, M.R., Dillingham, M.S., Wigley, D.B., 2007. Structure and mechanism of helicases and nucleic acid translocases. Annu. Rev. Biochem. 76, 23–50.
Sollars, E.S., Harper, A.L., Kelly, L.J., Sambles, C.M., Ramirez-Gonzalez, R.H., Swarbreck, D., Kaithakottil, G., Cooper, E.D., Uauy, C., Havlickova, L., Worswick, G., Studholme, D.J., Zohren, J., Salmon, D.L., Clavijo, B.J., Li, Y., He, Z., Fellgett, A., McKinney, L.V., Nielsen, L.R., Douglas, G.C., Kjær, E.D., Downie, J.A., Boshier, D., Lee, S., Clark, J., Grant, M., Bancroft, I., Caccamo, M., Buggs, R.J., 2017. Genome sequence and genetic diversity of European ash trees. Nature 541 (7636), 212–216.
Song, D., Cho, W.K., Park, S.H., Jo, Y., Kim, K.H., 2013. Evolution of and horizontal gene transfer in the endornavirus genus. PLoS One 8 (5), e64270. -e64270.
Sun, L., Nuss, D.L., Suzuki, N., 2006. Synergism between a mycoreovirus and a hypovirus mediated by the papain-like protease p29 of the prototypic hypovirus CHV1-EP713. J. Gen. Virol. 87 (12), 3703–3714.
Sun, Y., Li, J., Gao, G.F., Tien, P., Liu, W., 2018. Bunyavirales ribonucleoproteins: the viral replication and transcription machinery. Crit. Rev. Microbiol. 44 (5), 522–540.
Sutela, S., Poimala, A., Vainio, E.J., 2019. Viruses of fungi and oomycetes in the soil environment. FEMS Microbiol. Ecol. 95 (9), fiz119 https://doi.org/10.1093/femsec/fiz119.
Tuomivirta, T.T., Hantula, J., 2005. Three unrelated viruses occur in a single isolate of *Gremmeniella abietina* var. abietina type A. Virus Res. 110 (1–2), 31–39.
Tuomivirta, T.T., Kaitera, J., Hantula, J., 2009. A novel putative virus of *Gremmeniella abietina* type B (Ascomycota: helotiaceae) has a composite genome with endornavirus affinities. J. Gen. Virol. 90 (9), 2299–2305.
Urayama, S.-i., Katoh, Y., Fukuhara, T., Arie, T., Moriyama, H., Teraoka, T., 2014. Rapid detection of magnaporthe oryzae chrysovirus 1-A from fungal colonies on agar plates and lesions of rice blast. J. Gen. Plant Pathol. 81, 97–102.
Vainio, E.J., Chiba, S., Ghabrial, S.A., Maiss, E., Roossinck, M., Sabanadzovic, S., Suzuki, N., Xie, J., Nibert, M., 2018. ICTV virus taxonomy profile: *Partitiviridae*. J. Gen. Virol. 99 (1), 17–18.
Vainio, E.J., Pennanen, T., Rajala, T., Hantula, J., 2017. Occurrence of similar mycoviruses in pathogenic, saprotrophic and mycorrhizal fungi inhabiting the same forest stand. FEMS Microbiol. Ecol. 93 (3), fix003 https://doi.org/10.1093/femsec/fix003.
Valverde, R.A., Khalifa, M.E., Okada, R., Fukuhara, T., Sabanadzovic, S., Consortium, I. R., 2019. ICTV virus taxonomy profile: *Endornaviridae*. J. Gen. Virol. 100 (8), 1204–1205.
Wang, H., Li, C., Cai, L., Fang, S., Zheng, L., Yan, F., Zhang, S., Liu, Y., 2018. The complete genomic sequence of a novel botybirnavirus isolated from a phytopathogenic *Bipolaris maydis*. Virus Genes 54 (5), 733–736.
White, T.J., Bruns, T., Lee, S., Taylor, J., 1990. Amplification and direct sequencing of fungal ribosomal RNA genes for phylogenetics. PCR Protoc. Guide Methods Appl. 18 (1), 315–322.
Wu, M., Zhang, L., Li, G., Jiang, D., Ghabrial, S.A., 2010. Genome characterization of a debilitation-associated mitovirus infecting the phytopathogenic fungus *Botrytis cinerea*. Virology 406 (1), 117–126.
Yaegashi, H., Nakamura, H., Sawahata, T., Sasaki, A., Iwanami, Y., Ito, T., Kanematsu, S., 2013. Appearance of mycovirus-like double-stranded RNAs in the white root rot fungus, *Rosellinia necatrix*, in an apple orchard. FEMS Microbiol. Ecol. 83 (1), 49–62.
Yang, S., Dai, R., Salaipeth, L., Huang, L., Liu, J., Andika, I.B., Sun, L., 2021. Infection of two heterologous mycoviruses reduces the virulence of *Valsa mali*, a fungal agent of apple valsa canker disease. Front. Microbiol. 12, 659210.
Yao, W., Pan, J., Liu, Z., Dong, Z., Liang, M., Xia, S., Xiao, Y., Cai, X., Peng, T., Zhou, X., Cai, H., Flemington, E.K., Biron, C.A., 2021. The cellular and viral circRNAome induced by respiratory syncytial virus infection. mBio 12 (6), e03075.
Yu, X., Li, B., Fu, Y., Jiang, D., Ghabrial, S.A., Li, G., Peng, Y., Xie, J., Cheng, J., Huang, J., Yi, X., 2010. A geminivirus-related DNA mycovirus that confers hypovirulence to a plant pathogenic fungus. Proc. Natl. Acad. Sci. U. S. A. 107 (18), 8387–8392.
Zhang, R., Hisano, S., Tani, A., Kondo, H., Kanematsu, S., Suzuki, N., 2016a. A capsidless ssRNA virus hosted by an unrelated dsRNA virus. Nat. Microbiol. 1 (1), 15001.

Zhang, T., Jiang, Y., Huang, J., Dong, W., 2013. Genomic organization of a novel partitivirus from the phytopathogenic fungus *Ustilaginoidea virens*. Arch. Virol. 158 (11), 2415–2419.
Zhang, Y., Xue, W., Li, X., Zhang, J., Chen, S., Zhang, J.L., Yang, L., Chen, L.L., 2016b. The biogenesis of nascent circular RNAs. Cell Rep. 15 (3), 611–624.
Zhao, Y.J., Hosoya, T., Baral, H.O., Hosaka, K., Kakishima, M., 2013. *Hymenoscyphus pseudoalbidus*, the correct name for *Lambertella albida* reported from Japan. Mycotaxon 122 (1), 25–41.